Accuracy of Microwave Transistor fT and fMAX Extractions

Accuracy of Microwave Transistor f_{T} and f_{MAX} Extractions

Valeria Teppati, *Senior Member, IEEE,* Stefano Tirelli, Rickard Lövblom, Ralf Flückiger, Maria Alexandrova, and C. R. Bolognesi, *Fellow, IEEE*

***Abstract*—We present a complete methodology to evaluate the accuracy of microwave transistor figures-of-merit f_{T} (current gain cut-off frequency) and f_{MAX} (maximum oscillation frequency). These figures-of-merit are usually extracted from calibrated S-parameter measurements affected by residual calibration and measurement uncertainties. Thus, the uncertainties associated with f_{T} and f_{MAX} can be evaluated only after an accurate computation of the S-parameters uncertainties. This was done with the aid of two recently released software tools. In the uncertainty propagation, the standard de-embedding techniques are assumed to be error free, but still contributing to the final uncertainty budget with their measurement uncertainty. We also present an analysis on how different interpolation/extrapolation methodologies affect uncertainty. In addition, an overview of the possible causes of errors and suggestions on how to avoid them are given. With the continued rise of reported f_{T}/f_{MAX} values, this study has become necessary in order to evaluate the accuracy of these these figures-of-merit both by adding confidence intervals to their values and by identifying possible extraction errors.**

***Index Terms*—Integrated circuit measurements, measurement uncertainty, millimeter wave devices, millimeter wave technology, millimeter wave transistors.**

I. Introduction

ALTHOUGH a vast literature regarding uncertainty evaluation of S-parameter measurements exists [1]–[7] it was only recently that two software tools able to perform a complete uncertainty evaluation of S-parameter measurements – including covariance information – became available.

The tools in question are VNA Tools II [8], provided by the Swiss Metrological Institute (METAS) and available at [9] (SW1), and MMS4 [10], developed by HFE [11] (SW2).

These two tools differ profoundly in their approach and implementation, however, after a careful comparison presented in [12], it has been proven that they both provide consistent results as long as the input sources of uncertainty (noise, connection repeatability and standard uncertainty) are properly set. Because of their proven reliability, these tools can be used to compute the uncertainties of derived quantities. A relevant example is represented by the uncertainty propagation to f_{T} (current gain cut-off frequency) and f_{MAX} (maximum oscillation frequency) of a microwave transistor. Quantifying uncertainties is crucial in this case because these parameters are often used as benchmarks: to effectively compare results from different sources, one should take into account not only their absolute values, but also their associated uncertainties.

In general, the uncertainty of a derived quantity depends on the procedure used to compute the relevant quantities, in our case the S-parameters, starting from the raw data output from the instrument. This involves instrument calibration and additional computational steps to shift the reference planes closer to the Device Under Test (DUT) active area (de-embedding). Our work focuses on on-wafer devices, but the methodology we present can in principle be applied to any measurement environment.

This paper is structured as follows. Section II reports how S-parameter uncertainty is computed and propagated with full covariance matrices. Section III describes how uncertainties propagate through the de-embedding. Section IV deals with some general considerations about the propagation of uncertainties to f_{T} and f_{MAX} whereas Section V highlights the effect of using different parameters for the extraction. In Section VI, considerations on the possible causes of error are given, with suggestions on how to avoid them. Finally Section VII draws the conclusions to this work.

II. S-parameter Uncertainty Evaluation

The software tools used in this work to compute S-parameters uncertainty take into account the following contributions:

- Vector Network Analyzer (VNA) noise,
- Probe contact repeatability,
- Uncertainty of calibration standard definitions.

A thorough discussion on the evaluation of the three contributions listed above was presented in [12], and the results were applied to this work.

The VNA noise contribution was estimated by performing repeated VNA measurements, and was found to be typically negligible with respect to the other sources of uncertainty.

For what concerns probe repeatability, 40A-GSG-150-P and 110H-GSG-150 (Picoprobe) mounted on manual probe stations were characterized as described in [10]. For each standard, the probes were raised and lowered 20 times, each time changing slightly their position and the amount of overtravel, to achieve a good statistics for repeatability. The results are 1+v_T and v_R variances (as defined in [10], equation (32) and following) of 0.08 dB and -50 dB respectively at 40 GHz for the 40A-GSG-150-P and of 0.06 dB and -43 dB at 110 GHz for the 110H-GSG-150.

This work was partially funded by the Swiss National Science Foundation (SNSF), grant n. PMPDP2_139697, and carried out at the Millimeter Wave Electronics Laboratory (MWE), ETH Zurich, 8092 Zurich, Switzerland.

The authors are with the Department of Informationstechnologie und Elektrotechnik, ETH-Zurich, Zurich CH-8092, Switzerland (e-mail: bolognesi@mwe.ee.ethz.ch).

The last contribution, i.e. the uncertainty of the calibration standards, was defined by a-priori knowledge on the fabrication tolerances of the standards. This data is sometimes made available by the calibration substrate manufacturers or otherwise needs to be assumed on the basis of experience or previous measurements.

These contributions are taken into account by the two tools with an important difference. SW1 provides complete covariance matrices with correlation among different frequencies, whereas SW2 provides only correlation between the different S-parameters. The main contribution to frequency correlation is typically due the uncertainty of standard definition and is taken into account with SW1.

The subsequent propagation of the uncertainty was performed through the library tool Metas.UncLib [8], [13], [14] provided free of charge by METAS.

III. Uncertainty Propagation Through A Traditional Device De-Embedding

A common strategy to remove the parasitic effects of the interconnects between on-wafer probes and the active region of the DUT is to perform a de-embedding procedure after a VNA calibration at the probe tips. This is done using open and short structures, fabricated simultaneously with the DUT.

More complex de-embedding techniques, not considered in this paper [15], [16], can also involve thrus or loads.

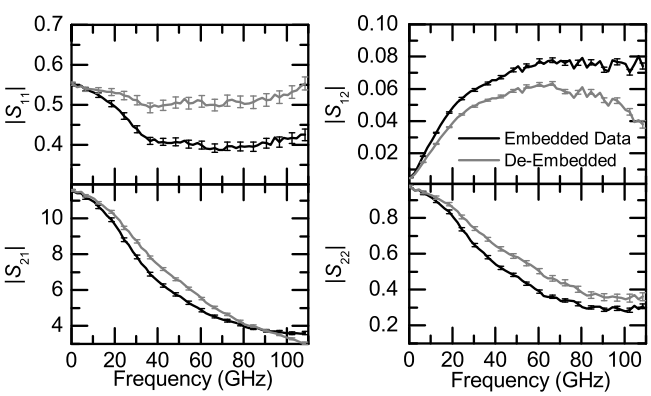

Fig. 1. Effect of the de-embedding on the calibrated S-parameters of a common-emitter InP DHBT, biased with 1.2 V collector-emitter voltage and with a base current of 400 μA (1σ uncertainty bars).

We focus on the most widely used de-embedding techniques, the so called open-short and short-open methods, respectively using

$$Z_{\mathrm{DUT,os}} = (Y_{\mathrm{DUT}} - Y_{\mathrm{O}})^{-1} - (Y_{\mathrm{S}} - Y_{\mathrm{O}})^{-1} \quad (1)$$

or

$$Y_{\mathrm{DUT,so}} = (Z_{\mathrm{DUT}} - Z_{\mathrm{S}})^{-1} - (Z_{\mathrm{O}} - Z_{\mathrm{S}})^{-1} \quad (2)$$

to compute the DUT impedance matrix $Z_{\mathrm{DUT,os}}$ or its admittance matrix $Y_{\mathrm{DUT,so}}$, where Y_{S} (Z_{S}), Y_{O} (Z_{O}) and Y_{DUT} (Z_{DUT}) are the short, open and DUT admittance (impedance) matrices, respectively.

A comparison of open-short de-embedded and non-de-embedded data for a common-emitter InP Double Heterojunction Bipolar Transistor (DHBT) is shown in Fig. 1. It can be noticed how de-embedding generally increases the uncertainty bars. In particular, for several analyzed data sets, it was found that the uncertainty on the de-embedded S-parameters S_{11}, S_{12} and S_{22} can increase by 20-50 % with respect to the non-de-embedded data, while the uncertainty on S_{21} (a typically larger quantity) might be even lower after de-embedding.

With these tools it is also possible to evaluate the uncertainty related to the fabrication of the de-embedding structures. A possible approach is to model the de-embedding structures with a lumped element equivalent circuit where each element value has an associated uncertainty. If resistive elements are left out from the model, f_{MAX} is practically insensitive to the uncertainty of the reactive embedding network elements. On the other hand, uncertainties on inductances and capacitances propagate to f_{T}, but are typically highly reduced. For example an uncertainty of 10 % on the reactive elements results in an uncertainty of 1-2 % on f_{T}.

IV. Uncertainty Propagation To f_{T} And f_{MAX}

A. Quantities of Interest Definition

The extraction process of f_{T} and f_{MAX} involves in all cases an elaboration of the measured S-parameters of the transistor, within a chosen frequency range and at a given bias point.

From common practice, it is well known that f_{T} and f_{MAX} are extremely sensitive to the type of calibration applied to compute the S-parameters and on the de-embedding strategy adopted. For example, as shown in [17], up to 10% difference on f_{MAX} can be observed using different calibration types.

The following analysis quantifies how f_{T} and f_{MAX} are affected by the measurement uncertainty, taking into account for the first time the complete covariance matrices of the input S-parameters of the DUT and the de-embedding structures.

The extraction is performed from the following quantities:

- Transmission hybrid parameter (H_{21}),
- Unilateral gain (U),
- Maximum Stable Gain (MSG) if $k < 1$,
- Maximum Available Gain (MAG) if $k >= 1$,

where k is the stability factor (see Appendix A for the complete expressions). f_{MAX} is defined as the frequency at which U or MSG/MAG are equal to 0 dB. f_{T} is defined as the frequency point where the short-circuit current gain H_{21} is equal to 0 dB. An alternative definition for f_{T} is through the Gummel method [18] - where f_{T} is extracted from the inverse of the low frequency slope of $\mathrm{Im}\left\{\frac{1}{H_{21}}\right\}$.

Whatever method is used, f_{T}/f_{MAX} and their uncertainties depend in first place on whether a single frequency point or an interpolation/extrapolation of measured data, using $n > 1$ measured points are used.

B. Case 1: Single Point Approach

When f_{T} or f_{MAX} are already represented by a data point belonging to the measured set, the uncertainty of the quantity of interest is determined directly from the measurement uncertainty of that point. This is also the case when a single data point is used for the extraction, for example when f_{MAX}

is extracted from the highest frequency point because $k < 1$ over the entire measurement range. Alternatively, single-point determination of $f_{\mathrm{T}}/f_{\mathrm{MAX}}$ is also often used in manufacturing environments for the sake of expediency.

We now focus on how two popular calibration algorithms impact the results, while keeping the same extraction method, and give some typical figures for uncertainties.

The device considered for this comparison was an InP DHBT biased with 1.6 V collector-emitter voltage and a base current of 500 μA. f_{T} was computed by extrapolating the last measured frequency point (40 GHz) of H_{21} with a -20 dB/decade slope as a function of frequency, and f_{MAX} by extrapolating the last measured frequency point of U, in a similar way, with a -20 dB/decade slope.

Table I reports the results obtained for f_{T} and f_{MAX} using a Short Open Load Reciprocal (SOLR) and a Thru Reflect Match (TRM) calibration. The intermediate results obtained before open-short (OS) or short-open (SO) de-embedding are also shown. It can be noted that the two calibrations are metrologically compatible, as uncertainty intervals always overlap, even if they do not give always the same results.

TABLE I
f_{T} AND f_{MAX} MEAN VALUES AND UNCERTAINTIES (1σ). THE UNCERTAINTY VALUES IN BOLD ARE COMPUTED NEGLECTING PROBE REPEATABILITY. VALUES IN GHZ.

	TRM	SOLR
f_{MAX} (no de-emb.)	414 $\pm$ 12 (**2**)	391 $\pm$ 20 (**5**)
f_{MAX} (OS de-emb.)	428 $\pm$ 16 (**2**)	428 $\pm$ 27 (**7**)
f_{MAX} (SO de-emb.)	432 $\pm$ 19 (**3**)	454 $\pm$ 34 (**9**)
f_{T} (no de-emb.)	389 $\pm$ 6 (**1**)	382 $\pm$ 11 (**3**)
f_{T} (OS de-emb.)	410 $\pm$ 9 (**1**)	409 $\pm$ 17 (**4**)
f_{T} (SO de-emb.)	405 $\pm$ 9 (**1**)	412 $\pm$ 17 (**4**)

It was found that neglecting probe repeatability reduces the uncertainties dramatically (see Table I, values in bold). As expected, de-embedding increased the uncertainty and SOLR algorithm showed larger uncertainties than the TRM in all cases.

C. Case 2: Multiple Points Approach.

When more frequency points are used to compute f_{T} or f_{MAX}, the uncertainty heavily depends on the number of points used for the interpolation/extrapolation, and on the correlation between the various points, whereas the extracted f_{T} or f_{MAX} value often changes just slightly.

As an example, we focus on the computation of f_{MAX} for a GaN HEMT, which is performed by interpolating measurement data in a range close to the actual f_{MAX} value. The uncertainty associated with multiple point extraction for a DHBT will be shown in Section V.

The measured MAG and U with their associated 1σ uncertainties are shown in Fig. 2. In the 90-110 GHz range, MAG and U coincide, as well as their uncertainties, and the data fits well to a -20 dB/decade slope line. The estimated value for f_{MAX} was consistently found to lie between 110 and 112 GHz. When the covariance matrices between the different frequency points were neglected, the uncertainty dropped from 5.2 (one point) to 1.2 GHz (40 points). This is

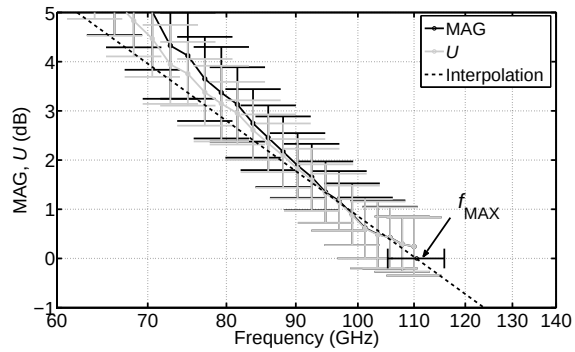

Fig. 2. MAG (black) and U (grey) with uncertainty (1σ). The interpolating line (dashed) was computed in the range 90-110 GHz, with 20 points (only a subset of the actually measured points is shown). The result of this extraction and its uncertainty, $f_{\mathrm{MAX}} = (110.5 \pm 5.3)$ GHz, is also shown.

mainly due to the mean operation involved when considering more than one point. When correlation was taken into account, the uncertainty increased to a more realistic value of 5.4 GHz. As expected, multiple points extractions require covariance information between different frequency points. This information is provided by SW1 and not by SW2, which in this case may underestimate the uncertainty.

V. UNCERTAINTY DEPENDENCE ON THE EXTRACTION PARAMETER

f_{T} and f_{MAX} can be extracted from different device parameters, each having different sensitivities to measurement uncertainty. The final f_{T} and f_{MAX} uncertainties are affected by the choice of the extraction parameter, as will be shown in this Section.

In the following, we compare the results obtained for an InP DHBT and a GaN HEMT. The DHBT was measured at $I_{\mathrm{B}} = 400\ \mu$A and $V_{\mathrm{CE}} = 1.2$ V while the HEMT was measured at $V_{\mathrm{GS}} = -0.75$ V and $V_{\mathrm{DS}} = 5$ V. The S-parameters of the DHBT are those reported in Fig. 1.

A. f_{T} Uncertainty

Fig. 3 shows H_{21} and $\mathrm{Im}\left\{\frac{1}{H_{21}}\right\}$, for the two transistors.

For the HEMT, the uncertainty of H_{21} rapidly increases for low frequency. The reason appears clear by looking at the denominator of H_{21}, see equation (A.4) in Appendix A.

At low frequencies, while S_{21} at the numerator remains finite, the denominator goes to zero, because S_{11} tends to 1 and S_{12} vanishes. Therefore, H_{21} goes to infinity and so does its derivative. The increase in the derivative reflects on the rapid increase of the uncertainty.

For the DHBT under test, S_{11} is almost constant (~ 0.55 in magnitude for the entire measurement range, as can be seen in Fig. 1), while for the HEMT S_{11} tends to one for low frequency.

$\mathrm{Im}\left\{\frac{1}{H_{21}}\right\}$, shown in Fig. 3(b), has a similar behavior for both the HEMT and the DHBT. In this case, we find a reversed behavior with respect to the uncertainty of H_{21}. The uncertainty of its imaginary inverse increases as S_{21} tends to zero, i.e. typically for high frequency (or low S_{21} transistors).

Table II summarizes the extracted f_{T} values and their uncertainties, obtained with the different methods for the

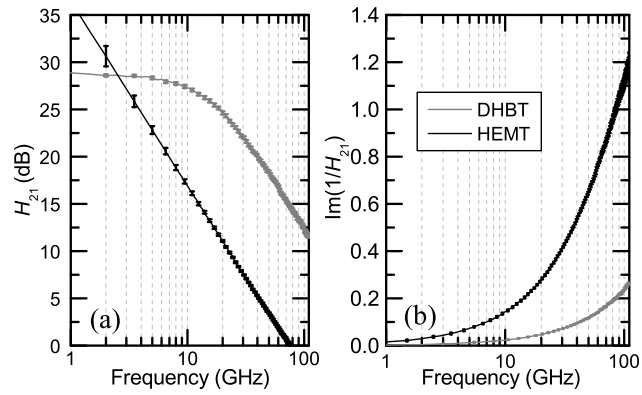

Fig. 3. H_{21} (a) and $\mathrm{Im}\left\{\frac{1}{H_{21}}\right\}$ (b) typical behavior for an InP DHBT and a GaN HEMT, with uncertainty (1σ).

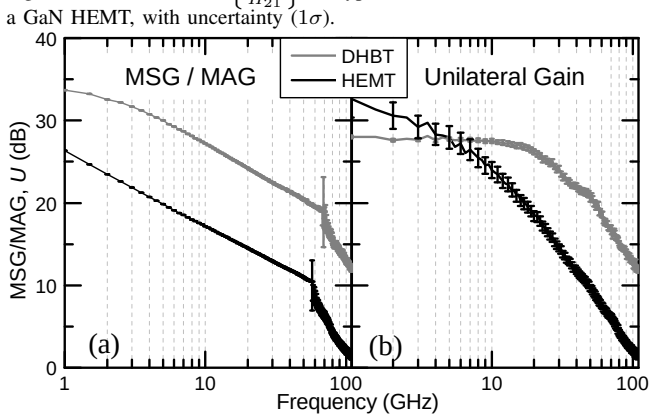

Fig. 4. MSG/MAG (a) and U (b) typical behavior for an InP DHBT and a GaN HEMT, with uncertainty (1σ).

two transistors. For H_{21} of the DHBT, a -20 dB/dec linear fit was chosen as extrapolation method, using the highest frequency points (80-110 GHz, 31 points). For the HEMT, no extrapolation was needed as f_{T} is included in the measurement frequency range. f_{T} was extracted by simply interpolating the two points closest to the $|H_{21}|$ zero crossing. The chosen extrapolation ranges for the Gummel method were 1 to 15 GHz for the DHBT and 0 to 5 GHz for the HEMT. In general, it was found that this method has a higher uncertainty and can be affected by large errors, strongly depending on the interpolation range.

B. f_{MAX} Uncertainty

Fig. 4 shows a comparison of the behavior of U and MSG/MAG, for the same GaN HEMT and InP DHBT.

The U parameter uncertainty has a completely different behavior for the two transistors. The reason, as for f_{T}, is that the S_{11} parameter of the HEMT tends to one as frequency decreases. For frequencies above 40 GHz, U tends to have the same uncertainty level for both transistors.

TABLE II
$f_{\mathrm{T}}/f_{\mathrm{MAX}}$ AND THEIR UNCERTAINTY (1σ) FOR AN INP DHBT AND A GAN HEMT, WITH DIFFERENT METHODS. VALUES IN GHZ.

	f_{T} (H_{21})	f_{T} (Gummel)	f_{MAX} (MSG/MAG)	f_{MAX} (U)
DHBT	418 ± 4	424 ± 12	432 ± 11	440 ± 12
HEMT	76 ± 1	70 ± 5	129 ± 5	129 ± 5

The uncertainty of the low frequency data points has an impact on the final uncertainty budget when these are also included in the model to extract f_{MAX}. This happens, e.g., if a one-pole function is used to approximate the curve over the entire frequency range. For a transistor with a large S_{11} (> 0.9) it is therefore better to use a high frequency extrapolation/interpolation.

For what concerns MSG/MAG, shown in Fig. 4(a), the uncertainties of the HEMT and the DHBT have a similar trend; when $k > 1$ (above 60 GHz), an abrupt change in the uncertainty occurs. The reason becomes evident by comparing the definitions of MAG and MSG, given in equations (A.3) of Appendix A. MSG depends only on S_{21} and S_{12}; MAG depends also on the stability factor, adding its uncertainty to the final uncertainty budget.

However, even if the MSG uncertainty is typically very low, if f_{MAX} is extracted with a -20 dB/dec line through its last data point, e.g. because of a limitation of the measured frequency range, the extracted value of f_{MAX} may be affected by significant error, as will be shown in the next Section.

Finally, by comparing Fig. 4(a) and 4(b), one can see that the uncertainty levels of MAG and U are similar. As a consequence, the extracted f_{MAX} will also have the same uncertainty with the two methods, as shown by Table II which reports the values obtained with an extrapolation at -20 dB/decade of the high frequency points (80-110 GHz, 31 points). Fig. 2 provides another example of this behavior, consistently found in all the measured transistors.

VI. POSSIBLE CAUSES OF ERROR

We now discuss certain conditions that can lead to significant errors in the extraction of $f_{\mathrm{T}}/f_{\mathrm{MAX}}$.

First we consider errors depending on the choice of the range used for the extrapolation and on extrapolation type.

Fig. 5 shows a typical situation for a GaN HEMT. In general, problems can arise when the extraction is performed extrapolating data in the frequency range where the stability factor k is close to 1, or the slope has not reached the nominal -20 dB/dec value [19], [20]. In the considered example, significant errors are made if the extraction is performed in the range 38-85 GHz (between the vertical dashed lines in Fig. 5). If measurements are stopped at $\sim$64 GHz, f_{MAX} will be 158 GHz, instead of 110 GHz. Even the extraction of f_{MAX} from U can be critical. A relevant error would be introduced if measurements were performed only up to 40 GHz, with $f_{\mathrm{MAX}} = 140$ GHz and an overestimation of 30 GHz with respect to the actual value. Therefore, for an accurate estimation of f_{MAX}, both the uncertainties and the behavior of the DUT within the available measurement range must be taken into account.

Also the choice of the extrapolation method is crucial and leads to different results. A typical critical situation is when the available frequency range is not sufficiently extended to reach the region where the extrapolating parameter has a well defined slope. The H_{21} of the DHBT in Fig. 3 is a good example. Its behavior is clearly that of a 1-pole function, which can be used for the fitting instead of a -20 dB/dec line. Even when

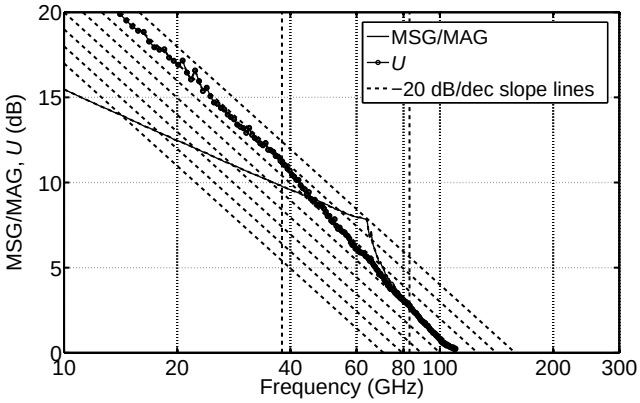

Fig. 5. Typical behavior of MSG/MAG and U versus frequency of a GaN HEMT. If the highest frequency data point lies between the vertical dashed lines (i.e. the range 38-85 GHz) the extracted value would largely overestimate f_{MAX}.

this is done, residual error is made if the measurement range is reduced. Table III reports the values of f_{T} obtained with the two extrapolation functions, for different frequency ranges. The 1-pole fitting causes a relatively small error in excess (7 GHz) when measurements are stopped at 40 GHz, while the -20 dB/dec fitting causes a large error, underestimating f_{T} by 35 GHz.

TABLE III
f_{T} OF THE INP DHBT OF SECTION V (FIG. 3), EXTRACTED FROM DIFFERENT FREQUENCY RANGES AND EXTRAPOLATION TYPES. VALUES IN GHZ.

1-pole fit range	f_{T}	-20 dB/dec extrap. range	f_{T}
0-40	433	30-40	391
0-67	431	40-67	412
0-110	426	80-110	418

In addition to these errors, a reliable estimate of f_{T} and f_{MAX} must also take into account the suitability of the extrapolation with respect to the transistor behavior. Deviations from the -20 dB/dec slope can arise due to device behavior, especially for very high f_{MAX} [21], [22], and this can be as well considered as a source of error.

Another possible critical situation is the one depicted in Fig. 6, where data is digitized from [23] and [24]. The U data show a recurrent "resonance" pattern for measurements performed on different devices, at different times. Ripple in U data (spikes of 4-5 dB) can considerably affect f_{MAX} extraction. Unless this error is somehow removed, it can actually be considered and treated as uncertainty. In such a case, the measurement uncertainty due to VNA noise, contact repeatability and standard definition as considered in the present paper, appears to be a second order effect.

Since f_{MAX} was extracted with a single-pole least-square fit of the data, a possible estimation of uncertainty in such a case could be given by the following expression:

$$\delta U = \sqrt{\frac{1}{n-1}\sum_{i=1}^{n}|U_i - p_i|^2} \tag{3}$$

where n is the number of samples, U_i is the ith sample and p_i is the value of the single pole least square fit on sample i.

The dotted lines in Fig. 6 represent the single pole least square fit, while dashed line represent its uncertainty bounds computed with (3). The extracted f_{MAX} is then (775 $\pm$ 130) GHz for [23] (with δU = 1.4 dB) and (885 $\pm$ 100) GHz for [24] (with δU = 1 dB).

Finally, as also shown in [25], another possible cause of error is due to de-embedding inaccuracies. This can be easily recognized when the open-short (1) and short-open (2) techniques start to give different results (typically for frequencies exceeding 50 GHz). For an accurate evaluation of $f_{\mathrm{T}}/f_{\mathrm{MAX}}$ this error must be corrected, e.g. by increasing the number of cascaded de-embedding sections in the extrinsic parameter model, as proposed in [25], or via more complex de-embedding strategies, as for example [15], [16]. An analysis of how different de-embedding techniques can lead to different results was presented in [26].

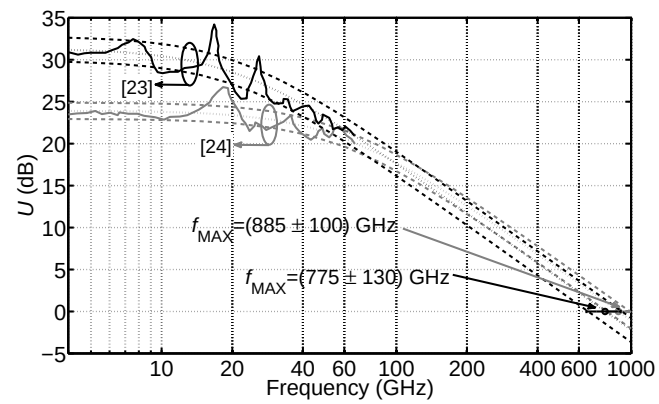

Fig. 6. A possible critical situation for f_{MAX} extraction. Data was digitized from [23] and [24]. Dotted lines represent a single pole least square fit, while dashed lines represent uncertainty bounds computed with (3).

VII. CONCLUSIONS

We presented the first complete evaluation of the accuracy of microwave transistors f_{T} and f_{MAX}. The uncertainty was propagated from the measured S-parameters of the DUT and de-embedding structures, using two recently released software tools. We identified the major contributions to the uncertainties and proved that covariance information between different frequencies is crucial for a proper evaluation. Errors and uncertainties due to different extrapolation methods were analyzed in details, identifying the most critical extraction conditions. The presented analysis allows for a consistent benchmarking of modern microwave transistors, especially as f_{T} and f_{MAX} reach increasingly high values.

APPENDIX A

We report here the expressions of the the quantities of interest MSG, MAG, k, H_{21} and U in terms of the device S-parameters. The stability factor k is

$$k = \frac{1 - |S_{11}|^2 - |S_{22}|^2 + |S_{11}S_{22} - S_{12}S_{21}|^2}{2|S_{12}S_{21}|} \tag{A.1}$$

and the Unilateral Gain is expressed as

$$\mathrm{U} = \frac{1}{2}\frac{\left|\frac{S_{21}}{S_{12}} - 1\right|^2}{k\left|\frac{S_{21}}{S_{12}}\right| - \mathrm{Re}\left(\frac{S_{21}}{S_{12}}\right)}. \tag{A.2}$$

MAG and MSG are expressed as

$$\mathrm{MAG} = \left(k - \sqrt{k^2 - 1}\right)\left|\frac{S_{21}}{S_{12}}\right|, \quad \mathrm{MSG} = \left|\frac{S_{21}}{S_{12}}\right|. \quad \text{(A.3)}$$

Finally, the hybrid parameter H_{21} is:

$$H_{21} = \frac{-2S_{21}}{(1 - S_{11})(1 + S_{22}) + S_{12}S_{21}}. \quad \text{(A.4)}$$

Appendix B

A thorough propagation of the uncertainty with frequency covariance, as the one shown in this work, always provides the most accurate and reliable results. However, for quick and practical estimation of the uncertainty of an extracted cut-off frequency f_x, we introduce a "rule of thumb" based on the following simplified assumptions:

- the extraction of f_x is performed using a -20 dB/decade slope interpolation/extrapolation of measured points,
- the points considered for the interpolation/extrapolation all have the same δy_{dB} uncertainty (expressed in dB),
- the measured frequency points are perfectly correlated.

Under these assumptions we can approximate the uncertainty of f_x with the following expression:

$$\delta f_x = \pm f_x \left(10^{\frac{\delta y_{dB}}{20}} - 1\right). \quad \text{(B.1)}$$

With this expression, the relative uncertainty $\frac{\delta f_x}{f_x}$ is ± 3 % for $\delta y_{dB} = \pm 0.25$ dB and ± 6 % for $\delta y_{dB} = \pm 0.5$ dB. Table IV shows some results for absolute uncertainty.

TABLE IV
UNCERTAINTY "RULE OF THUMB".

f_x (GHz)	δf_x (GHz) for $\delta y_{dB} = \pm 0.25$ dB	δf_x (GHz) for $\delta y_{dB} = \pm 1$ dB
50	$\pm$ 1.5	$\pm$ 6
200	$\pm$ 6	$\pm$ 25
400	$\pm$ 12	$\pm$ 49
800	$\pm$ 23	$\pm$ 98
1000	$\pm$ 30	$\pm$ 122

Acknowledgments

The authors wish to thank the developers of the software tools used in this work, Marco Garelli (HFE) and Michael Wollensack (METAS), for their help and support.

References

[1] A. M. E. Safwat and L. Hayden, "Sensitivity analysis of calibration standards for SOLT and LRRM," in *58th ARFTG Microwave Measurements Conference*, San Diego, CA, Nov. 2001, pp. 1–10.

[2] N. Ridler and M. Salter, "A generalised approach to the propagation of uncertainty in complex S-parameter measurements," in *64th ARFTG Microwave Measurements Conference*, Orlando, FL, Dec. 2004, pp. 1–14.

[3] J. Martens, "LRM: a quantitative look at reference impedance contradictions and other uncertainty impacts," in *69th ARFTG Microwave Measurements Conference*, Honolulu, HI, June 2007, pp. 1–7.

[4] A. Rumiantsev, P. Corson, S. Sweeney, and U. Arz, "Applying the calibration comparison technique for verification of transmission line standards on silicon up to 110 GHz," in *73rd ARFTG Microwave Measurements Conference*, Boston, MA, June 2009, pp. 1–6.

[5] A. Lewandowski, D. Williams, P. Hale, C. M. Wang, and A. Dienstfrey, "Covariance-matrix-based vector-network-analyzer uncertainty analysis for time-and frequency-domain measurements," *IEEE Trans. Microwave Theory Tech.*, vol. MTT-58, no. 7, pp. 1877–1866, July 2010.

[6] U. Stumper and T. Schrader, "Influence of different configurations of nonideal calibration standards on vector network analyzer performance," *IEEE Trans. Instr. Meas.*, vol. 61, no. 7, pp. 2034–2041, July 2012.

[7] A. Arsenovic, L. Chen, M. F. Bauwens, H. Li, N. S. Barker, and I. R. M. Weikle, "An experimental technique for calibration uncertainty analysis," *IEEE Trans. Microwave Theory Tech.*, vol. 61, no. 1, pp. 263–269, Jan. 2013.

[8] M. Zeier, J. Hoffmann, and M. Wollensack, "Metas.UncLib – a measurement uncertainty calculator for advanced problems," *Metrologia*, vol. 49, no. 6, p. 809, 2012. [Online]. Available: http://stacks.iop.org/0026-1394/49/i=6/a=809

[9] M. Wollensack and J. Hoffmann. (2012, Apr.) METAS VNA Tools II - Math Reference. [Online]. Available: www.metas.ch/vnatools

[10] A. Ferrero and M. Garelli, "A unified theory for S-parameter uncertainty evaluation," *IEEE Trans. Microwave Theory Tech.*, vol. MTT-60, no. 12, pp. 3844–3855, Dec. 2012.

[11] HFE Sagl, Multiport S-parameters Software - MMS4. [Online]. Available: www.hfemicro.com

[12] V. Teppati and A. Ferrero, "A comparison of uncertainty evaluation methods for on-wafer S-parameter measurements," *IEEE Trans. Instr. Meas.*, vol. PP, no. 99, accepted for publication.

[13] M. Wollensack and M. Zeier. (2011, Nov.) Metas.UncLib - An advanced Measurement Uncertainty Calculator. [Online]. Available: www.metas.ch/unclib

[14] B. D. Hall, "Calculating measurement uncertainty using automatic differentiation," *Measurement Science and Technology*, vol. 13, no. 4, p. 421, 2002. [Online]. Available: http://stacks.iop.org/0957-0233/13/i=4/a=301

[15] M.-H. Cho, G.-W. Huang, C.-S. Chiu, K.-M. Chen, and A.-S. Peng, "A Cascade Open-Short-Thru (COST) de-embedding method for microwave on-wafer characterization and automatic measurement," *IEICE Trans. Electron.*, vol. E88-C, no. 5, pp. 845–850, May 2005.

[16] I. M. Kang, S.-J. Jung, T.-H. Choi, J.-H. Jung, C. Chung, H.-S. Kim, H. Oh, H. W. Lee, G. Jo, Y.-K. Kim, H.-G. Kim, and K.-M. Choi, "Five-step (padpad shortpad openshortopen) de-embedding method and its verification," *IEEE Electron Device Letters*, vol. 30, no. 4, pp. 398–400, Apr. 2009.

[17] *Calibration Tools - Consistent Parameter Extraction for Advanced RF Devices*, Application Note, CascadeMicrotech®, 2012.

[18] H. Gummel, "On the definition of the cutoff frequency ft," *Proceedings of the IEEE*, vol. 57, no. 12, pp. 2159–2159, 1969.

[19] L. Nguyen, P. Tasker, and W. Schaff, "Comments on "A new low-noise AlGaAs/GaAs 2DEG FET with a surface undoped layer"," *Electron Devices, IEEE Transactions on*, vol. 34, no. 5, pp. 1187–1187, 1987.

[20] P. Roblin and H. Rohdin, *High-speed heterostructure devices*, Cambridge University Press, Cambridge, UK, 2002.

[21] M. Vaidyanathan and D. Pulfrey, "Extrapolated fmax of heterojunction bipolar transistors," *Electron Devices, IEEE Transactions on*, vol. 46, no. 2, pp. 301–309, 1999.

[22] A. Laser and D. Pulfrey, "Reconciliation of methods for estimating fmax for microwave heterojunction transistors," *Electron Devices, IEEE Transactions on*, vol. 38, no. 8, pp. 1685–1692, 1991.

[23] Z. Griffith, E. Lind, M. J. W. Rodwell, X.-M. Fang, D. Loubychev, Y. Wu, J. Fastenau, and A. Liu, "Sub-300 nm InGaAs/InP Type-I DHBTs with a 150 nm collector, 30 nm base demonstrating 755 GHz f_{MAX} and 416 GHz f_{T}," in *Indium Phosphide Related Materials, 2007. IPRM '07. IEEE 19th International Conference on*, 2007, pp. 403–406.

[24] E. Lobisser, Z. Griffith, V. Jain, B. J. Thibeault, M. J. W. Rodwell, D. Loubychev, A. Snyder, Y. Wu, J. Fastenau, and A. Liu, "200-nm InGaAs/InP type I DHBT employing a dual-sidewall emitter process demonstrating $f_{\mathrm{MAX}} >>$ 800 GHz and f_{T} = 360 GHz," in *Indium Phosphide Related Materials, 2009. IPRM '09. IEEE International Conference on*, 2009, pp. 16–19.

[25] L. F. Tiemeijer and R. J. Havens, "A calibrated lumped-element de-embedding technique for on-wafer RF characterization of high-quality inductors and high-speed transistors," *IEEE Trans. Electron Devices*, vol. 50, no. 3, pp. 822–829, Mar. 2003.

[26] J. Cha, J. Cha, and S. Lee, "Uncertainty analysis of two-step and three-step methods for deembedding on-wafer RF transistor measurements," *IEEE Trans. Electron Devices*, vol. 55, no. 8, pp. 2195–2201, Aug. 2008.